Giant magnetoresistance in a two-dimensional electron gas modulated by magnetic barriers

2004 J. Phys.: Condens. Matter 16 8275

(http://iopscience.iop.org/0953-8984/16/46/014)

INSTITUTE OF PHYSICS PUBLISHING JOURNAL OF PHYSICS: CONDENSED MATTER

J. Phys.: Condens. Matter **16** (2004) 8275–8283 PII: S0953-8984(04)83549-5

Giant magnetoresistance in a two-dimensional electron gas modulated by magnetic barriers

G Papp[1,2,3] **and F M Peeters**[3]

[1] Department of Theoretical Physics, University of Szeged, Aradi Vértanúk tere 1, H-6720 Szeged, Hungary
[2] Institute of Physics, University of West Hungary, Bajcsy Zsilinszky út 5-7, H-9400 Sopron, Hungary
[3] Departement Fysica, Universiteit Antwerpen (Campus Drie Eiken), Universiteitsplein 1, B-2610 Antwerpen, Belgium

E-mail: pgy@physx.u-szeged.hu and francois.peeters@ua.ac.be

Received 15 July 2004, in final form 20 October 2004
Published 5 November 2004
Online at stacks.iop.org/JPhysCM/16/8275
doi:10.1088/0953-8984/16/46/014

Abstract

The temperature-dependent giant magnetoresistance effect is investigated in a magnetically modulated two-dimensional electron gas, which can be realized by depositing two parallel ferromagnets on the top and bottom of a heterostructure. The effective potential for electrons arising for parallel magnetization allows the electrons to resonantly tunnel through the magnetic barriers, while this is excluded in the anti-parallel situation. Such a discrepancy results in a giant magnetoresistance ratio (MRR), which can be up to $10^{31}\%$. The MRR shows a strong dependence on temperature, but our study indicates that for realistic parameters for a GaAs heterostructure the effect can be as high as $10^{4}\%$ at 4 K.

1. Introduction

The patterning of ferromagnetic materials integrated with semiconductors allows one to create magnetic barriers, magnetic wells, magnetic dot structures, and periodic and quasiperiodic magnetic superlattices [1]. The magnetic barrier system [2] is very different from the well-known potential barrier because the electron tunnelling is now a two-dimensional (2D) problem. The transmission depends not only on the energy of the impeding electrons but also on the direction in which the electrons move towards the barrier.

The discovery of the so-called giant magnetoresistance (GMR) effect [3] has given rise to a tremendous economic impact on magnetic information storage [4]. Fueled by its fascinating practical applications such as ultrasensitive magnetic field sensors, read heads, and random access memories, numerous theoretical and experimental studies are dealing with the GMR phenomenon [5]. The structures where GMR is observed generally consist of ferromagnetic

layers separated by thin non-magnetic layers. In such heterogeneous systems, GMR is characterized by a striking drop of the electric resistance when an external magnetic field switches the magnetization of adjacent magnetic layers from an antiparallel (AP) alignment to a parallel (P) one. To obtain a large MRR, an attractive alternative is to use magnetic or superconducting microstructures on the surface of heterostructures containing a two-dimensional electron gas (2DEG). Microstructured ferromagnets (or superconductors) provide an inhomogeneous magnetic field which influences locally the motion of the electrons in the semiconductor. Nogaret *et al* [6] demonstrated a new type of MRR at low temperature in a hybrid ferromagnetic/semiconductor device, and an MRR of up to $10^3\%$ at 4 K was observed [7].

The spin-independent GMR effect was studied by Zhai *et al* [8] in a magnetically modulated two-dimensional electron gas, which can be realized by depositing two parallel ferromagnets on top of a heterostructure. The authors found that the transmission for parallel and antiparallel magnetization shows a quite distinct dependence on the longitudinal wavevector of the incident electrons, resulting in a tremendously large zero-temperature magnetoresistance ratio $(G_{\rm P} - G_{\rm AP})/G_{\rm AP}$, which can be up to $10^6\%$ for realistic electron densities. The MRR can be further tuned by the inclusion of an electric barrier. It was recently shown by us [9] that the giant magnetic resistance effect is significantly reduced when the temperature is not zero. Furthermore, in practical devices not only the MRR but also the MMR ratio, i.e. $(G_{\rm P} - G_{\rm AP})/(G_{\rm P} + G_{\rm AP})$, is a relevant quantity which was found to have a less spectacular behaviour.

In the present paper we propose an alternative way to realize the GMR effect. The considered system is a two-dimensional electron gas (2DEG) in the (x, y) plane modulated by a perpendicular magnetic field B_z. Our system is schematically depicted in figure 1, where metallic ferromagnetic stripes are deposited on the top and bottom of a heterostructure. When a magnetic field is directed parallel to the 2DEG the magnetic materials become magnetized parallel to the 2D plane, which leads to fringing fields near the edge of the magnetic materials having a non-homogeneous magnetic field component perpendicular to the 2DEG (as for example was demonstrated experimentally in [10]). The fringe field of the upper ferromagnet induces a positive B_z underneath one edge of the stripe and a negative B_z underneath the other edge (dashed curves in figures 1(b), (c) [11]), and similarly for the ferromagnet at the bottom (dotted curves in figures 1(b), (c)). A suitable external parallel magnetic field can change the relative orientation of the two magnetizations (dotted curves in figure 1(b)). For small distances between the 2DEG and the ferromagnets, the magnetic barrier can be approximated by delta functions, i.e.,

$$B_z(x) = Bl_{\rm B}\left\{\mathrm{sgn}(x)\left[\delta\left(|x| - \frac{w}{2}\right)\chi - \delta\left(|x| - d - \frac{w}{2}\right)\right]\right\}.$$

Here, B gives the strength of the magnetic field, $l_{\rm B} = \sqrt{\hbar c/eB_0}$ is the magnetic length for an estimated magnetic field B_0, $\mathrm{sgn}(x)$ is the sign function, χ represents the magnetization configuration ($\chi = +1$ for P and $\chi = -1$ for AP), w is the width of the bottom ferromagnetic stripe, and $w + 2d$ is the width of the top ferromagnetic stripe along the current direction (x). The model magnetic field configurations for the parallel (P) and anti-parallel (AP) configurations are schematically depicted in figures 1(c) and (b), respectively.

The present paper is organised as follows. In section 2 we give the Schrödinger equation of our system, and show how it transforms to an effective 1D problem. The numerical results and our discussions are presented in section 3 and the conclusions are given in section 4.

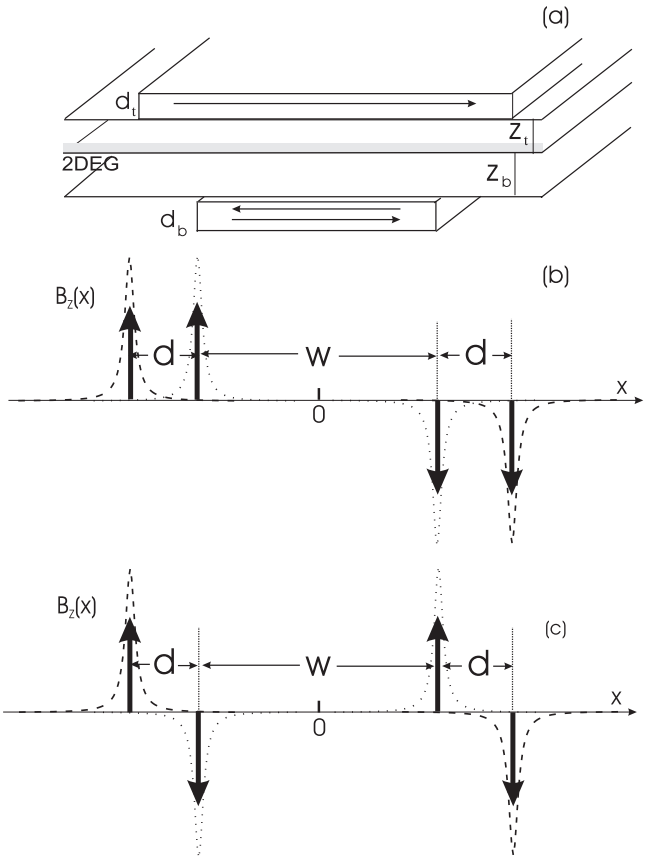

Figure 1. (a) Schematic illustration of the device: magnetic stripes are placed on the top and bottom of a 2DEG. Theoretical model for the magnetic field profile for the anti-parallel (b) and parallel (c) configurations of the two magnetic stripes. In (b) and (c) the dashed and dotted curves are the real magnetic field profile and the solid arrows are the ones used in our model.

2. Theoretical model

We consider a two-dimensional electron gas moving in the (x, y)-plane in the presence of the inhomogeneous magnetic field profiles depicted in figures 1(b), (c). Our magnetic field is of the form $\mathbf{B} = B_z(x)\mathbf{e}_z$. The δ-function magnetic field profile is an approximation for the real fringe fields of the ferromagnets and we assume that the effect of the parallel magnetic field component on the electron can be neglected. In previous papers [1, 12] it was shown that such a δ-function approximation is sufficiently accurate in order to obtain qualitatively correct estimates for the tunnelling properties. The Hamiltonian describing such a system, in the single particle effective mass approximation, is

$$H = \frac{p_x^2}{2m^*} + \frac{(p_y + \frac{e}{c}A_y(x))^2}{2m^*} + \frac{eg^*}{2m_0}\frac{\sigma_z\hbar}{2c}B_z(x), \tag{1}$$

where m^* is the effective mass, and m_0 the free electron mass, (p_x, p_y) is the electron momentum, and g^* is the effective Landé-factor of the electron in the 2DEG. $\sigma_z = +1/-1$ for spin-up/spin-down electrons, and the magnetic vector potential of our magnetic barriers case can be written as $(0, A_y(x), 0)$ in the Landau gauge. Because the system is translationally

invariant along the y-direction the solution of the stationary Schrödinger equation $H\Psi(x, y) = E\Psi(x, y)$ can be written as a product $\Psi(x, y) = e^{ik_y y}\psi_{\sigma_z}(x)$, where $\hbar k_y$ is the expectation value of the momentum p_y in the y-direction. The wavefunction $\psi_{\sigma_z}(x)$ satisfies the following 1D Schrödinger equation:

$$\left[\frac{d^2}{dx^2} - \left(k_y + \frac{e}{c\hbar}A_y(x)\right)^2 + \frac{2m^*}{\hbar^2}\left\{E - \frac{eg^*}{2m_0}\frac{\sigma_z\hbar}{2c}B_z(x)\right\}\right]\psi_{\sigma_z}(x) = 0. \quad (2)$$

If we introduce the following characteristic parameters [2]: $\omega_c = eB_0/m^*c$ with B_0 some typical magnetic field, and l_B the corresponding magnetic length, the Schrödinger equation becomes

$$\left[\frac{d^2}{dx^2} + 2(E - V(x, k_y))\right]\psi_{\sigma_z}(x) = 0, \quad (3)$$

where all quantities are expressed in dimensionless units: $x \to l_B x$, $E \to \hbar\omega_c E$ and

$$V(x, k_y) = \frac{(k_y + A_y(x))^2}{2} + \frac{g^* m^* \sigma_z B_z(x)}{4m_0}, \quad (4)$$

with $A_y \to B_0 l_B A_y$, $B_z(x) \to B_0 B_z(x)$ and $k_y \to k_y/l_B$. The problem is now reduced to a one-dimensional (1D) tunnelling problem. The 1D potential $V(x, k_y)$ depends on the wavevector k_y, the relative arrangement of the magnetic stripes, and also on the interaction between the non-homogeneous magnetic field and the electron spin. The A_y is zero to the left and right of the field region in both the P and AP cases, and the y-component of the electron momentum in these incident and transmitted regions is determined just by k_y. The effective potentials are depicted in figure 2 for two values of k_y in the case of anti-parallel magnetization (a), and parallel magnetization (b). From figure 2 or from the expression of the vector potential $A_y(x) = -B[\Theta(\frac{w}{2} - |x|)\chi - \Theta(d + \frac{w}{2} - |x|)]$, one can see that when the P alignment ($\chi = +1$) turns to the inverse ($\chi = -1$), $V(x, k_y)$ varies substantially. It is this dependence of the magnetic profile of $V(x, k_y)$ on the relative alignment of the ferromagnets that leads to the GMR in the considered system. The last term in equation (4) represents the Zeeman coupling between the electronic spin and the local magnetic field.

Following [2] we calculated the electric current through the two-dimensional electron gas, in the ballistic regime. The conductance G is obtained as the electron flow averaged over half the Fermi surface[4] [13]:

$$G = 2G_0 \sum_{\sigma=-1,1} \int_{-\frac{\pi}{2}}^{\frac{\pi}{2}} T\left(E_F, \sqrt{2E_F}\sin\phi\right)\cos\phi\, d\phi, \quad (5)$$

where ϕ is the angle of incidence relative to the x-direction, $G_0 = e^2 m^* v_F L_y/h^2$ [14][5], where L_y is the length of the structure in the y-direction and v_F is the Fermi velocity.

3. Results and discussions

In our numerical calculation the material parameters were taken for the GaAs system where the electron effective mass is $m^*_{GaAs} = 0.067m_0$ and the effective Landé-factor $g^*_{GaAs} = 0.44$. We take typically for GaAs $n_e \approx 10^{11}$ cm^{-2}, which gives $E_F = 3.55$ meV, and use $B_0 = 0.2$ T, which is a realistic value. This leads to the units $l_B = 575$ Å, and $E_0 = \hbar\omega_c = 0.34$ meV.

Figure 3 presents the transmissions for P and AP alignment when the spin–magnetic field interaction is neglected for (a) $k_y = -2$ and (b) $k_y = 0$ and 2. The effective potential

[4] This equation was derived in [2b] (see equation (6)) and is based on the Landauer–Büttiker formula.
[5] The expression of G_0 in equation (6) of [2b] should be divided by $2\pi^2$.

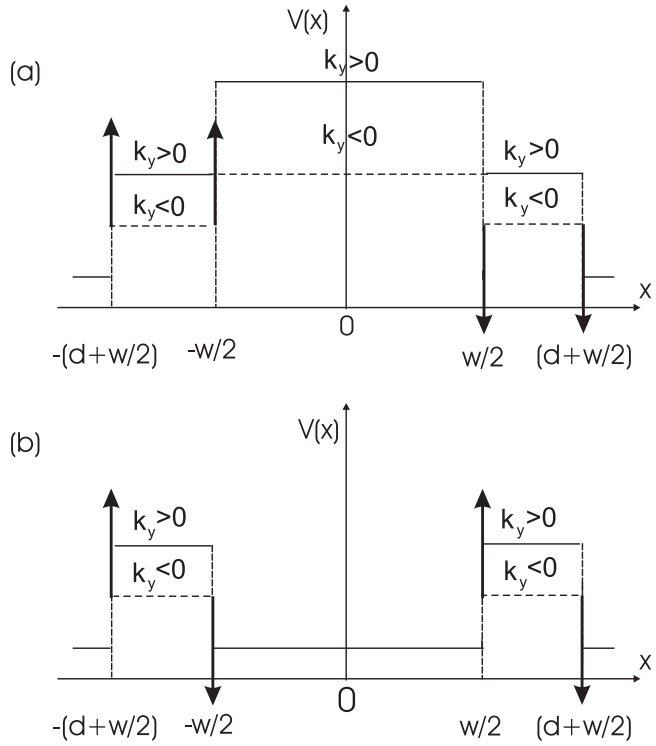

Figure 2. The effective potential for different k_y values for anti-parallel (a) and parallel (b) magnetization of the two ferromagnetic stripes in figure 1.

resulting from the magnetic barriers, in the case of P alignment and for values of k_y which are larger than $-B/2$ (in dimensionless units), consists of quantum-barriers and where the bottom ferromagnet acts as a quantum well. Consequently the transmission behaviour is similar to resonant tunnelling through a double-barrier quantum-well structure. This is clearly seen in figure 3, where the transmission probability is shown for $B = 5$, $d = 1$ and $w = 3$. For both k_y values there exist several sharp resonant peaks of height unity corresponding to resonant tunnelling. The latter occurs when the incident energy coincides with one of the quasibound energy levels within the well. For barriers lower than the first intrawell virtual state, however, no resonance appears when the energy falls below the barriers. The magnetic barriers, for values of k_y which are less than $-B/2$, behave as symmetric double wells, which are usually transparent for electrons. The magnetic barriers, in the case of AP alignment for values of k_y which are larger than $-B/2$, also behave as quantum barriers, but the region of the bottom ferromagnet now acts as a quantum barrier but with a height twice as large (figure 2(a)), which is clearly reflected in the transmission. The transmission is blocked and resonant tunnelling is excluded. Even for values of k_y which are less than $-B/2$, they behave as a barrier, and only when $k_y < -B$ do they behave as a quantum well. From these facts one can conclude that, for a given incident energy, only electrons with negative k_y values have non-zero transmission through the same structure with AP arrangement. Therefore, such a device can be used as a momentum filter for the 2D electrons.

In the 2DEG system modulated by the two FM stripes with their magnetizations along the x-direction (parallel or anti-parallel alignment), the Hamiltonian is invariant [12] under

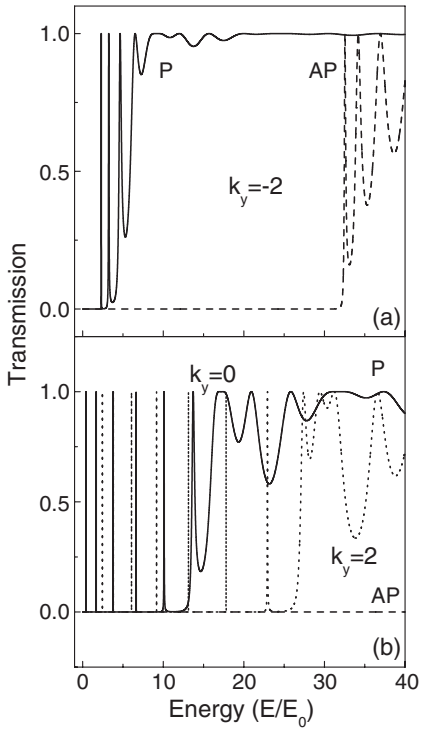

Figure 3. The transmission probability for spinless electrons tunnelling through magnetic barriers with parallel (P) and anti-parallel (AP) magnetization as a function of energy for (a) $k_y = -2$ and (b) $k_y = 0$ (solid curve) and $k_y = 2$ (dotted curve) for P configuration, and $k_y = 0$ (dashed curve) for AP configuration. The magnetic structure parameters are $B = 5$, $d = 1$, and $w = 3$ (see figure 1(a)).

the operation $\hat{T}\hat{R}_x\hat{R}_y$, where $\hat{T} = -\mathrm{i}\hat{\sigma}_y K$ with K being the complex conjugate time-reversal operator, and $\hat{R}_x$ ($\hat{R}_y$) is the reflection operator $x \to -x$ ($y \to -y$). This symmetry implies that states with wavefunctions $\Psi(x, y) = \mathrm{e}^{\mathrm{i}k_y y}\psi_{\sigma_z}(x)$ and $\Psi'(x, y) = \hat{T}\hat{R}_x\hat{R}_y\Psi(x, y)$ have the same eigenenergy and consequently the same tunnelling properties. It can be easily verified that under the operation of $\hat{T}\hat{R}_x\hat{R}_y$, a spin-up state $\mathrm{e}^{\mathrm{i}k_y y}\psi_\uparrow(x)$ transforms to a spin-down state $\mathrm{e}^{\mathrm{i}k_y y}\psi_\downarrow(x)$, and a spin-down state $\mathrm{e}^{\mathrm{i}k_y y}\psi_\downarrow(x)$ transforms to a spin-up state, $\mathrm{e}^{\mathrm{i}k_y y}\psi_\uparrow(x)$. Thus the spin-up and spin-down states with the same wavevector k_y are degenerate, and the transmission probability is spin direction independent: $T(E, k_y, \sigma_z) = T(E, k_y, -\sigma_z)$. As a result, there is no spin polarization in the electron transport through the system in the linear response regime. When the spin–magnetic field interaction is included the transmission probability is altered for all values of the energy, especially at the resonant energies. The resonant peaks shift to lower energy for the spin-up electron but this shift is more pronounced for the P alignment. The electronic spin and the local magnetic field interaction depend on the quantity $g^*Bm^*/2m_0$. For $B = 5$ the value of the latter is 0.0737 for GaAs, which is much smaller then E_F/E_0 and therefore we will neglect the spin-dependent part in the subsequent discussion.

Having seen the transmission results, one may wonder to what extent their structure is reflected in measurable quantities, which often involve some kind of averaging. In figure 4(a) we show the conductance versus the Fermi energy, as calculated using equation (5). For comparison, we drew the curve of P and AP conductance normalized with respect to $2G_0$.

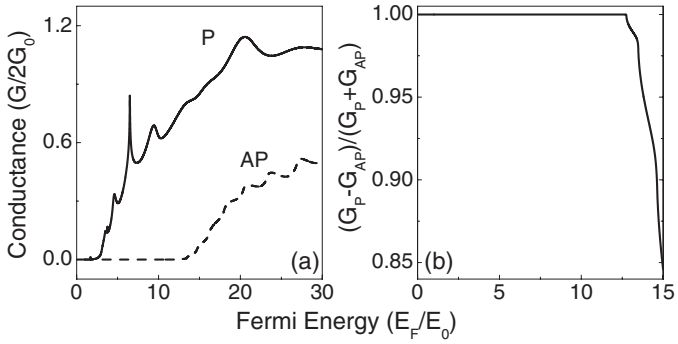

Figure 4. The conductance (a), and the modified magnetic resistance ratio (b) as a function of the Fermi energy. The magnetic structure parameters are the same as those in figure 3.

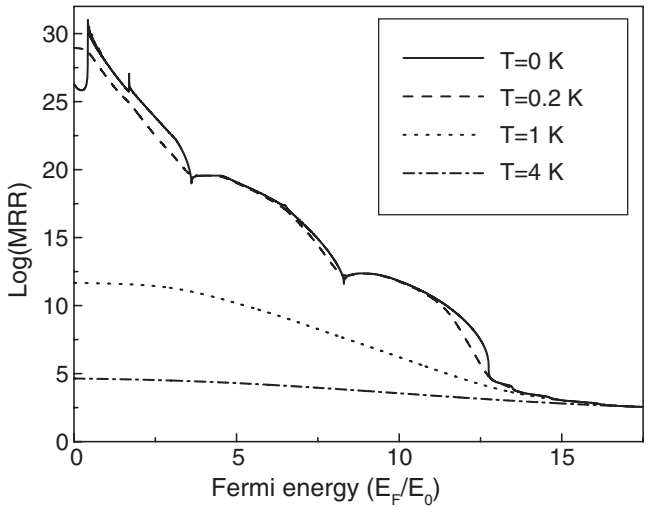

Figure 5. The logarithm of the MRR versus the Fermi energy for different temperature: $T = 0$ K (solid curve), $T = 0.2$ K (dashed curve), $T = 1$ K (dotted curve) and $T = 4$ K (dash–dotted curve). The magnetic structure parameters are the same as those in figure 3.

Notice the large difference in conductance between the P and AP alignments. G_{P} has for low Fermi energies some peaks (due to the sharp transmission peaks in the resonance tunnelling region), and exhibits a rapid increase at low energies (this is absent in G_{AP}). In addition, the G_{P} curve has a striking conductance peak with a large peak-to-valley ratio (i.e. for $E_{\mathrm{F}}/E_0 \simeq 6.5$) as well as several small peaks. The reason is that for electrons with negative k_y value the resonant tunnelling interval is smaller [9] and these electrons together with the resonant tunnelling electrons incident with a positive k_y component lead to the peaks in the conductance. For the AP alignment the magnetic barrier blocks the transmission drastically and the corresponding conductance is almost zero. So there exists a wide energy region where G_{AP} is close to zero whereas G_{P} is finite. That feature is illustrated by the modified magnetic resistance ratio which is shown in figure 4(b). To see the discrepancy between G_{P} and G_{AP} more clearly, we present in figure 5 the logarithm of the magnetoresistance ratio as a function of the Fermi energy (solid curve). Notice that for low temperature the MRR $= (G_{\mathrm{P}}/G_{\mathrm{AP}} - 1)^*100(\%)$ has a fine structure as function of the Fermi energy and only when E_{F} exceeds $15E_0$ does

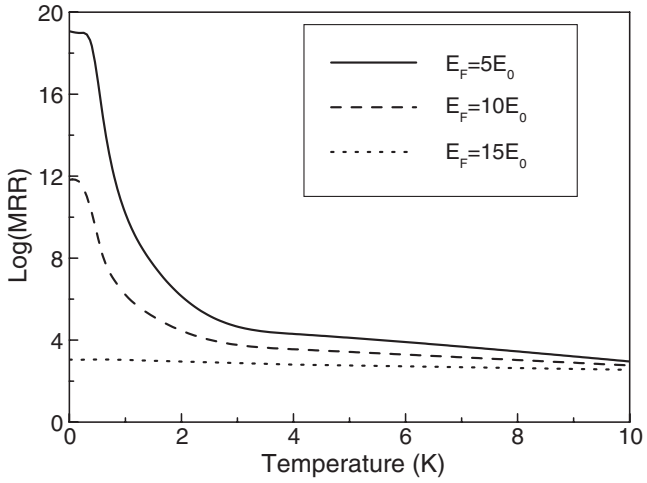

Figure 6. The logarithm of the MRR as a function of temperature for different values of the Fermi energy. The magnetic structure parameters are the same as those in figure 3.

the MRR decay to the magnitude of $10^3\%$. To generalize our results to non-zero temperature we have to replace any function of $G(E_F)$, which depends on the Fermi energy E_F, by the corresponding average over the derivative of the Fermi function: $G(\mu) = \int d\varepsilon\, G(\varepsilon)(-\frac{\partial f_0}{\partial \varepsilon})$, where $f_0 = \{\exp[(\varepsilon - \mu)/k_B T] + 1\}^{-1}$ and μ is the chemical potential. Figure 5 shows the logarithm of the magnetoresistance ratio for $T = 0.2$ K (dashed curve), $T = 1$ K (dotted curve), and $T = 4$ K (dash–dotted curve). For a typical electron density $n_e \approx 10^{11}$ cm^{-2} in a GaAs 2DEG which gives $E_F = 3.55$ meV $\approx 10E_0$, the corresponding MRR is about $10^{11}\%$ at very low temperature, which decreases to $3.10^3\%$ for $T = 4$ K and is 190 (184)% for 77 (300) K. For an electron density of $n_e \approx 4 \times 10^{11}$ cm^{-2} we find $E_F = 14.2$ meV $\approx 42E_0$ and an MRR of 71% for $T = 4$ K. The high value of the giant magnetic resistance is due to the definition of MRR, since it contains in its denominator the factor G_{AP}, which is much smaller than G_P. The physical reason is the strong suppression of the transmission in the AP alignment. The effect of temperature is to broaden the peak in the MRR to lower Fermi energy. In figure 6 the logarithm of the MRR is given as a function of temperature for different Fermi energies. Notice that even for $T = 4$ K there is still a significant difference between the P and AP alignment, resulting in a substantial MRR.

4. Conclusions

In the usual GMR devices electrical current is flowing through the ferromagnets and the layer between the two ferromagnets. The resistance changes are a consequence of the difference in magnetization orientation dependence of the resistance for spin-up and spin-down electrons. This is different in the present device, where current flows only through the heterostructure which is parallel to the ferromagnets and it is the direction dependence of the stray fields of the ferromagnets which are used to manipulate the electron current. The spin of the electron is only of secondary importance, and the main effect is based on the orbital effect of the magnetic field on the electron.

In conclusion, we have shown that electric transport, based on the tunnelling of two-dimensional electrons through magnetic barriers, results in a giant magnetic resistance effect

at low temperature. The magnetic barriers result from the stray field of ferromagnetic stripes deposited on the top and bottom of a heterostructure which are magnetized along the current direction. Our theoretical results indicate that the difference in ballistic transmission for two magnetization configurations (P versus AP) leads to a tremendous MRR, which can approach 10^{31}% at zero temperature. The ferromagnets just generate a modulated local field here, and electronic spin plays a minor role in the ballistic transport because of the small effective g^*-factor in the GaAs 2DEG. The MRR significantly changes when the temperature is not zero. But even at 4 K we found an MRR of 10^4% in the case of a GaAs heterostructure.

Acknowledgments

Part of this work was supported by the Flemish Science Foundation (FWO-Vl), the Belgian Science Policy, and the Flemish–Hungarian bilateral programme.

References

[1] For a recent review see for example Peeters F M and De Boeck J 1999 *Handbook of Nanostructured Materials and Nanotechnology* vol 3, ed H S Nalwa (New York: Academic) p 345
[2a] Peeters F M and Matulis A 1993 *Phys. Rev.* B **48** 15166
[2b] Matulis A, Peeters F M and Vasilopoulos P 1994 *Phys. Rev. Lett.* **72** 1518
[3] Baibich M N, Broto J M, Fert A, Nguyen Van Dau F, Petroff F, Etienne P, Creuzet G, Friederich A and Chazelas J 1988 *Phys. Rev. Lett.* **61** 2472
[4] Prinz G A 1998 *Science* **282** 1660
[5] For a review, see Levy P M 1994 *Solid State Phys.* **47** 367
Gijs M A M and Bauer G E W 1997 *Adv. Phys.* **46** 285
AnSermet J-Ph 1998 *J. Phys.: Condens. Matter* **10** 6027
[6] Nogaret A, Carlton S, Gallagher B L, Main P C, Henini M, Wirtz R, Newbury R, Howson M A and Beaumont S P 1997 *Phys. Rev.* B **55** R16037
[7] Overend N, Nogaret A, Gallagher B L, Main P C, Henini M, Marrows C H, Howson M A and Beaumont S P 1998 *Appl. Phys. Lett.* **72** 1724
Overend N, Nogaret A, Gallagher B L, Main P C, Wirtz R, Newbury R, Howson M A and Beaumont S P 1998 *Physica* B **249–251** 326
Nogaret A, Overend N, Gallagher B L, Main P C, Henini M, Marrows C H, Howson M A and Beaumont S P 1998 *Physica* E **2** 421
[8] Zhai F, Guo Y and Gu B-L 2002 *Phys. Rev.* B **66** 125305
[9] Papp G and Peeters F M 2004 *Physica* E at press
[10] Kubrak V, Rahman F, Gallagher B L, Main P C, Henini M, Marrows C H and Howson M A 1999 *Appl. Phys. Lett.* **74** 2507
Vančura T, Ihn T, Broderick S, Ensslin K, Wegscheider W and Bichler M 2000 *Phys. Rev.* B **62** 5074
[11] Reijniers J and Peeters F M 1998 *Appl. Phys. Lett.* **73** 357
[12] Zhai F, Xu H Q and Guo Y 2004 *Phys. Rev.* B **70** 085308
[13] Büttiker M 1986 *Phys. Rev. Lett.* **57** 1761
[14] Matulis A and Peeters F M 2000 *Phys. Rev.* B **62** 91